

# Update to Proposal E12-06-105

## Inclusive Scattering from Nuclei at $x > 1$ in the quasielastic and deeply inelastic regimes

Argonne National Laboratory  
University of Virginia  
Hampton University  
James Madison University  
Thomas Jefferson National Accelerator Facility  
University of New Hampshire  
University of Maryland  
University of Tennessee  
Yerevan Physics Institute, Armenia

John Arrington and Donal Day, co-spokespersons

(Dated: July 1, 2010)

E12-06-105 was approved to make measurements of inclusive scattering from nuclei at  $x > 1$ . There are two separate motivations for these measurements, corresponding to two different kinematic regions. Data at moderate  $Q^2$  but very large  $x$  ( $x > 1.3-1.5$ ) are dominated by quasielastic scattering from extremely high momentum nucleons, and is sensitive to the high-momentum tail of the nucleon distribution in nuclei. The distribution of high momentum nucleons is related to the short range structure and nucleon–nucleon correlations in nuclei. Data at much larger  $Q^2$  for  $1 \lesssim x \lesssim 1.5$  are dominated by DIS scattering from the  $x \gtrsim 1$  part of the nuclear parton distributions, and can be used to probe the distribution of these exceptionally high momentum quarks. The distribution of these “super-fast quarks” in nuclei is sensitive to short range structure in nuclei, including the possible contribution of non-hadronic components, such as six-quark bags.

This document provides a brief update to and a summary of the original proposal for E12-06-105 [1]. The scientific case for E12-06-105 has been strengthened by our ongoing analysis of E02-019. There we clearly see the indications of a transition from kinematics that dominated by quasielastic scattering to those dominated by deep inelastic scattering, strongly supporting the idea that the 11 GeV measurement will be able to provide a clean extraction of the nuclear pdfs at  $x > 1$ . In addition, the results from E03-013, which suggest that the size of the EMC effect is strongly correlated with the local nuclear density, led us to include additional light targets ( ${}^6,7\text{Li}$ ,  ${}^{10,11}\text{B}$ ) to the runplan for the study of short-range correlations, which are a direct measure of the amount of short distance, two-nucleon interaction. Finally, the results of E02-019 demonstrated that short cryotargets complicate the subtraction of the end-cap contributions, and so we will use 8 cm cells rather than the 4 cm cells from the original proposal and take additional time for the  $x \approx 3(4)$  settings for  ${}^3\text{He}$  and  ${}^4\text{He}$ . This additional running time, along with the time required for the additional light nuclei, is very close to the time saved by using the longer He cells for the remaining kinematics, and thus does not impact our beam time request.

### I. INTRODUCTION

Previous measurements of inclusive scattering from nuclei have been made for a range of targets at SLAC [2, 3] and at 4 and 6 GeV at JLAB [4–9]. These data have been important sources of information on the momentum distribution of nucleons in nuclei, with an emphasis on high-momentum nucleons and  $y$ -scaling studies that are sensitive to the reaction mechanism and have allowed for tests of various theoretical models of inclusive scattering.

The proposed measurements at large  $x$  ( $x \gtrsim 1.5$ ) at moderate  $Q^2$  values ( $\approx 2-3$  (GeV/c) $^2$ ) are dominated by quasielastic scattering from high momentum nucleons (momenta in excess of 1 GeV/c for the kinematics of this proposal), and can provide several important extensions to these studies. The cross section of few-body nuclei allow comparisons with essentially exact calculations of nuclear wave functions and provide an important complement to the coincidence  $A(e, e'p)$  and  $A(e, e'NN)$

measurements already completed or approved. Data on heavy nuclei will allow extrapolation to nuclear matter where again rigorous calculations can be performed and compared to the data.

Measurements of target ratios can be used to isolate and study the nature of the short range correlations (SRCs) that are the main source of the high momentum nucleons. We will have better  $Q^2$  and  $x$  coverage than previous measurements, and provide direct ratios of heavier nuclei to  $^2\text{H}$  and  $^3\text{He}$  to study 2-N and 3-N short range correlations, and a first look at  $x > 3$  in ratios to  $^4\text{He}$ . In addition, absolute cross section measurements in this region can help examine the microscopic structure of 3N correlations, as well as allowing us to examine the  $Q^2$  dependence of both the cross section and ratios to constrain final state interactions which can interfere with the interpretation in terms of correlations.

In addition to extending previous measurements of short range correlations, we will provide data at lower  $x$  but much higher  $Q^2$  values, where the cross section is dominated by deep inelastic scattering from quarks with  $x > 1$ . The quark distributions in nuclei at large  $x$  are poorly understood, and this will provide the first clean and unambiguous measurement of the distribution of so-called ‘‘superfast’’ quarks. These quark distributions provide an additional way to look for the effect of short range correlations, but also provide high sensitivity to non-hadronic components of nuclear structure in these high density, short range configurations within nuclei [10–12]. Using data from E02-109 we have already had some success in the extraction of the high  $x$  structure function distributions, as we will discuss below.

## II. HIGH MOMENTUM COMPONENTS AND SHORT RANGE CORRELATIONS

High energy electron scattering from nuclei can provide important information on the wave function of nucleons in the nucleus. With simple assumptions about the reaction mechanism, scaling functions can be deduced that should scale (*i.e.* become independent of length scale or momentum transfer) and which are directly related to the momentum distribution of nucleons in a nucleus. Several theoretical studies [13–16] have indicated that such measurements may provide direct access to short range nucleon-nucleon correlations.

While the observation of a  $y$ -scaling limit and the plateaus in the ratios of heavy nuclei to deuterium and  $^3\text{He}$  is suggestive of an approach to the impulse approximation limit, it is not definitive. Even if scaling is observed, that does not insure that the scaling function is directly connected to the momentum distribution. Some calculations [15, 17] have pointed out that while the FSI of a struck nucleon with the mean field of the rest of the nucleus is a rapidly decreasing function of  $Q^2$ , the FSI of the struck nucleon with a correlated, high-momentum nucleon may show a very weak  $Q^2$ -dependence.

One approach to this issue has been to focus on cross section ratios in the region where the scattering is expected to be dominated by short range correlations [10]. In the large  $x$  region where correlations should dominate,

$$\sigma(x, Q^2) = \sum_{j=2}^A A \frac{1}{j} a_j(A) \sigma_j(x, Q^2) = \frac{A}{2} a_2(A) \sigma_2(x, Q^2) + \frac{A}{3} a_3(A) \sigma_3(x, Q^2) + \dots,$$

where the constants  $a_j(A)$  are proportional to the probability of finding a nucleon in a  $j$ -nucleon correlation, which should fall rapidly with  $j$  as nuclei are dilute. So for  $1 < x < 2$ , the  $\sigma_2 = \sigma_{eD}$  term should dominate (as one expects  $a_3 \ll a_2$ ). Similarly, for  $2 < x < 3$ , one expects to be dominated

by three-nucleon SRCs. This picture neglects final state interactions (FSIs) and motion of the nucleons in the nucleus. However, while there can be  $Q^2$ -independent FSIs between the nucleons in the correlation, these should be nearly identical for correlations in light and heavy nuclei, and should cancel in the ratio  $\sigma_A/\sigma_D$ . The motion of the correlations will yield strength from a  $j$ -nucleon correlation extending slightly above  $x = (j - 1)$ , and thus one must stay somewhat above this region to isolate the correlation.

A combined analysis of several SLAC measurements at  $x > 1$  showed that in the region where two-nucleon SRCs were expected to dominate,  $1.5 \lesssim x < 2$ , the ratio of the cross section of heavier nuclei to deuterium was independent of  $x$  in this region and showed little  $Q^2$  dependence [18]. Measurements by the CLAS collaboration at Jefferson Lab [7] performed a similar analysis, taking ratios of  $^4\text{He}$ ,  $^{12}\text{C}$ , and  $^{56}\text{Fe}$  to  $^3\text{He}$  ( $^2\text{H}$  data were not available at these kinematics) in the region of 2N SRC dominance. The ratios were consistent with the SLAC results, and expanded the  $Q^2$  range, showing the effect of final state interactions at lower  $Q^2$  values (down to  $0.6 \text{ GeV}^2$ ), and providing measurements of the  $A/^3\text{He}$  ratios up to 2-2.5  $\text{GeV}^2$ . The data from E02-019 [6] also examined these ratios, providing measurements of the  $A/^2\text{H}$  ratios at much larger  $Q^2$  as seen in Fig. 1.

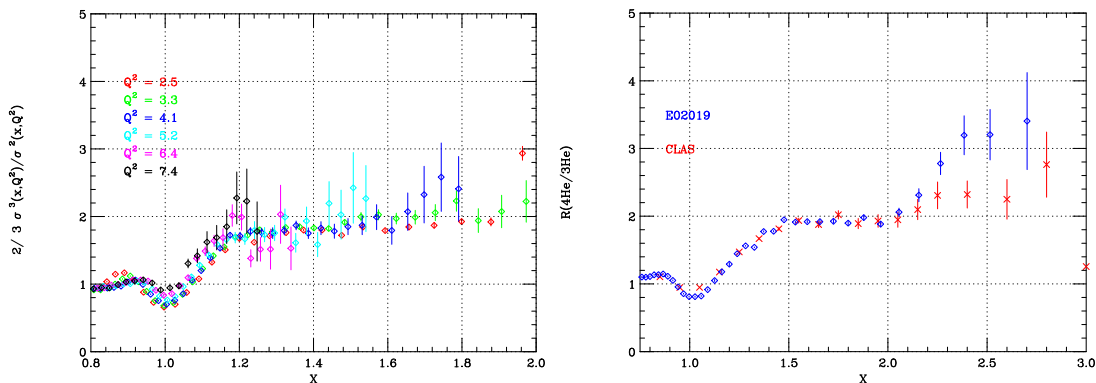


FIG. 1: Cross section ratios for  $^3\text{He}/^2\text{H}$  (left) at large  $x$  from from the Hall C measurements (E02019) for different  $Q^2$ . On the right is the ratio of  $^4\text{He}/^3\text{He}$  from both CLAS and E02019. The CLAS data is at  $1.4 < Q^2 < 1.6 \text{ GeV}^2$  and the E02019 data is at  $Q^2 \approx 2.5 \text{ GeV}^2$ .

This procedure was extended to the three-nucleon SRC region by a later CLAS measurement [8], which took an expanded data set and examined the  $A/^3\text{He}$  ratios up to  $x \approx 3$ . The ratios for this measurement were  $x$ -independent for  $2.25 < x < 3$ , consistent with the model of scattering from 3N SRCs. This very high  $x$  extraction is dominated by data with  $1.4 < Q^2 < 1.6 \text{ GeV}^2$ , and the extraction of the strength of 3N SRCs was made under the assumption that this  $Q^2$  was sufficient to yield scaling the 3N SRC region. The statistics were insufficient to provide a precise test of the  $Q^2$  independence of the ratio, although the extracted  $^{56}\text{Fe}/^3\text{He}$  ratio changes from  $R \approx 4$  for  $1.4 < Q^2 < 1.6 \text{ GeV}^2$  to  $R \approx 5.5$  for  $1.7 < Q^2 < 2.5 \text{ GeV}^2$ , as shown in Fig. 18 of Ref. [19]. Preliminary results from E02-019 show a similar plateau for  $x > 2.25$ , but the measurement is at  $Q^2 \approx 2.5 \text{ GeV}^2$ , and suggests a plateau that is significantly higher than the CLAS results at  $Q^2 \approx 1.5 \text{ GeV}^2$ , as shown in Fig. 1.

The measurements proposed here will have considerable advantages over the previous data:

1. In the 2N SRC region, we will take ratios of heavier nuclei directly to deuterium, rather than taking ratios to  $^3\text{He}$  and then using the SLAC global analysis of  $^3\text{He}$  and  $^2\text{H}$  measurements to

extract  $a_2$  (as was done in CLAS).

2. For  ${}^3\text{He}$ , we will make measurements at larger  $Q^2$ , with high statistical precision for  $2.25 \lesssim x < 3$ , allowing for a **detailed study of the scaling behavior in the  $A/{}^3\text{He}$  ratios**.
3. We will be able to examine the role of FSI through the  $Q^2$  **dependence of the ratios and absolute cross sections measurements** in the 2N correlation region ( $x > 1.5$ ).
4. Our ability to make precise **absolute cross section measurements in the 3N and 4N regions** will provide an opportunity to study the structure of the 3N correlations. The CLAS data measured only ratios, and E02-019 was statistics limited for  ${}^3\text{He}$  at  $x > 2.2$ .
5. We will include a range of nuclei, especially for  $A \leq 12$ , to map out in detail the A dependence in the 2N region, and make a first study of the A-dependence in the 3N region. Taking data with a wide variety of targets will provide an **insight to how non-isoscalarity manifests itself in the correlation region and how the local nuclear density contribute to SRC**.

While both CLAS and E02-019 provided data at  $x > 2$ , neither measurement mapped out the  $x$  or  $Q^2$  dependence with good precision. The disagreement between the results, as well as the statistics-limited  $Q^2$  dependence observed in the CLAS experiment, suggest that the ratios in the CLAS measurements may not have isolated the contribution of 3N SRCs. There is a 6 GeV approved experiment (E08-014 [20]) that focuses on  $x > 2$ . The experiment will map out the  $x$  and  $Q^2$  dependence with high precision, with the goal of defining the kinematic region where precise scaling behavior is observed. It will not map out the A dependence, as it will measure only  ${}^4\text{He}/{}^3\text{He}$ ,  ${}^{12}\text{C}/{}^3\text{He}$ , and  ${}^{48}\text{Ca}/{}^{40}\text{Ca}$ . In addition, if the scaling behavior does not set in until  $Q^2 = 2\text{--}2.5 \text{ GeV}^2$ , as suggested by the available data, then the measurements to be performed at  $6 \text{ GeV}^2$  will be able to observe the onset of scaling, but will not make precise measurements above  $x \approx 2.5$ . So E08-014 will be very valuable in defining the optimal kinematics for our detailed studies of 3N-SRCs, but will measure 3N SRCs for a very limited set of nuclei, and possibly over a limited range in  $x$ . While E08-014 will have data for  $x > 3$ , it will only be for their lower  $Q^2$  settings, and based on the current measurements for 3N SRCs, it seems unlikely that these data will be at sufficiently high  $Q^2$  to isolate 4N correlations.

### III. DEEP INELASTIC SCATTERING AT $x > 1$

The response of the nucleus in the range  $x > 1$  is composed of both inelastic scattering from quarks in the nucleus and elastic scattering from the bound nucleons (quasielastic scattering). Previous measurements of electron-nucleus scattering at  $x > 1$  have focussed on quasielastic scattering, and avoided regions where inelastic contributions have any significant contribution. The increase in energy to 11 GeV will allow us to make measurements at  $x > 1$  that are dominated by deeply inelastic scattering, allowing us to and map out the distribution of extremely high momentum nucleons in nuclei. Figure 2 shows the breakdown of the cross section for scattering at  $22^\circ$  and  $55^\circ$ , based on the convolution model described in [21]. At  $22^\circ$ , the data are dominated by DIS scattering only for  $x \lesssim 0.7$ , although it is dominated by inelastic scattering up to much larger  $x$  values. At  $55^\circ$ , the DIS contributions dominate up to  $x = 1.5$ .

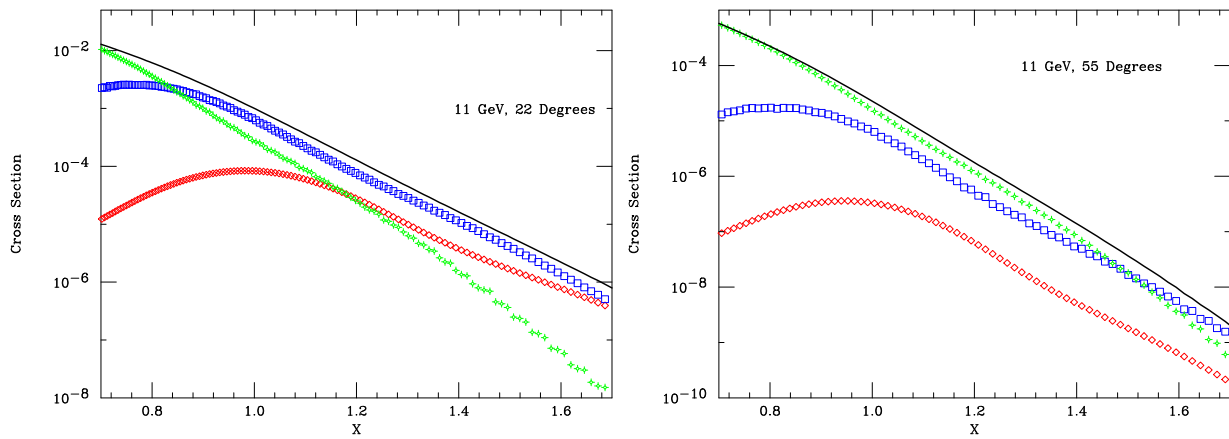


FIG. 2: Breakdown of the contributions to the inclusive cross section as a function of  $x$  for scattering at 11 GeV and 22° (left) and 55° (right) with and 11 GeV beam calculated in a convolution model [21]. The red diamonds indicate quasielastic contribution, the blue boxes show the contribution from the resonance region ( $W^2 < 4 \text{ GeV}^2$ ), and the green stars indicate the contribution from DIS scattering ( $W^2 > 4 \text{ GeV}^2$  in the photon-nucleon system).

It has been shown that a better connection can be made between the structure functions and the underlying quark distributions by using the Nachtmann scaling variable,  $\xi = 2x/(1 + \sqrt{1 + 4M^2x^2/Q^2})$  [22, 23]. In nuclei, significantly improved scaling is observed at large  $x$  when studying the  $Q^2$  dependence of  $F_2$  as a function of  $\xi$  rather than  $x$  (note that  $\xi \rightarrow x$  for  $Q^2 \rightarrow \infty$ ). These  $\xi$ -scaling analyses can be thought of as approximations to the application of target mass corrections, which account for scaling violation at finite  $Q^2$  values. Using the extended kinematic coverage of E02-019, we have performed a more detailed study [24] of the scaling of the structure function at large  $\xi$ . As a first step we applied the full “target mass” corrections, using the formalism of Ref. [25] to determine  $F_2^{(0)}(\xi, Q^2)$ , extracted from  $F_2$  using Eq.(23) from Ref. [25]:

$$F_2(x, Q^2) = \frac{x^2}{\xi^2 r^3} F_2^{(0)}(\xi, Q^2) + \frac{6M^2 x^3}{Q^2 r^4} h_2(\xi, Q^2) + \frac{12M^4 x^4}{Q^4 r^5} g_2(\xi, Q^2), \quad (1)$$

where  $h_2(\xi, Q^2) = \int_{\xi}^A u^{-2} F_2^{(0)}(u, Q^2) du$  and  $g_2(\xi, Q^2) = \int_{\xi}^A v^{-2} (v - \xi) F_2^{(0)}(v, Q^2) dv$ .

Calculation of the integrals  $h_2$  and  $g_2$  requires the use of a model for  $F_2^{(0)}(\xi, Q^2)$ . We make a simple global fit to the world’s data, in our kinematic range of  $x$  and  $Q^2$ , to provide a model for calculating  $h_2$  and  $g_2$ . This simple fit provides a reasonable description of the global data set (see Fig. 3), with deviations at low  $Q^2$ , in particular near the quasielastic peak ( $\xi \approx 0.85$ ) and for the largest values of  $\xi$ . We estimate the model dependence in the extraction of  $F_2^{(0)}$  to be  $\lesssim 2\%$ .

Figure 3 shows the carbon results for  $F_2^{(0)}(\xi, Q^2)$ , scaled to fixed values of  $\xi$ . For all data sets,  $F_2^{(0)}$  is extracted from the measured structure functions using the global fit to calculate  $g_2$  and  $h_2$ . The SLAC points are deuterium data [26], multiplied by the SLAC E139 [27] fit to the carbon-to-deuteron structure function ratio, yielding carbon pseudo-data to provide a continuous  $Q^2$  range for lower  $\xi$  values. For the lowest  $\xi$  value, the three data sets are in good agreement. At low  $Q^2$ , the data rise above the global fit in the vicinity of the quasielastic peak ( $\xi \approx 0.85$ ), while at very large  $\xi$  values, they fall below the fit. This is consistent with the  $\xi$ -scaling observation that the data approach the scaling limit from below as one increases  $Q^2$  [5, 28]. However, the highest  $Q^2$  data from the 6 GeV measurement seem to be consistent with the much higher  $Q^2$  data where it exists, suggesting that even at  $Q^2 \approx 7\text{--}9 \text{ GeV}^2$ , the data are consistent with the DIS scaling limit. With

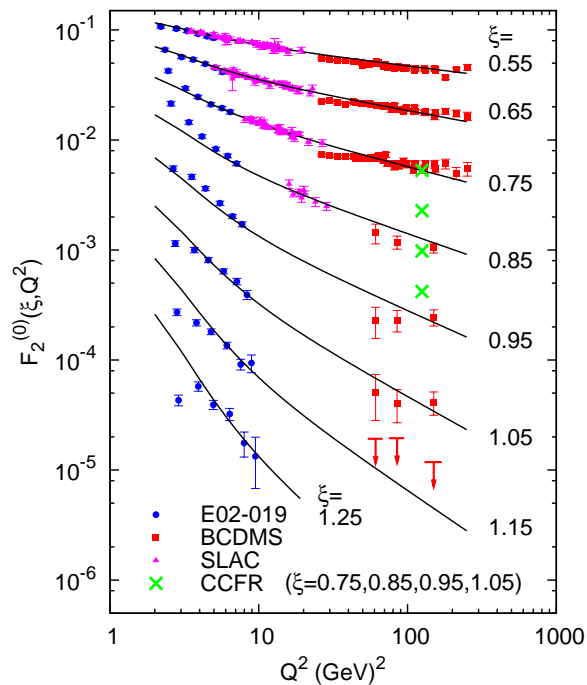


FIG. 3:  $F_2^{(0)}$  vs  $Q^2$  for fixed  $\xi$  value. For this work and BCDMS, the carbon data are shown, while the SLAC points are carbon pseudo-data taken from measurements on deuterium (see text). The solid curves are the global fit, used to calculate the  $h_2$  and  $g_2$  terms in the target mass corrections. The short horizontal red lines show the BCDMS  $\xi=1.15$  upper limit, and the green crosses show the falloff between  $\xi=0.75$  and  $\xi=1.05$  based on the CCFR data (see text for details).

the 11 GeV measurement, we will double the  $Q^2$  range, and should be able to extract the quark distributions over a significantly expanded range in  $\xi$ .

#### A. The distribution of superfast quarks

The data from E02-109 have given us a first chance to examine the  $\xi$ -dependence of the structure function for large values of  $\xi$  and compare to data measured at extremely high  $Q^2$  values ( $\sim 100$   $\text{GeV}^2$ ) in  $\mu$ -C scattering [29] and  $\nu$ -Fe scattering [30]. Near  $\xi = 1$ , these experiments obtained significantly different results. The neutrino experiment (CCFR) found  $F_2^{Fe} \propto \exp(-8.3x)$  (at these  $Q^2$ , the difference between  $\xi$  and  $x$  is relatively small), consistent with a significant contribution from superfast quarks in the nucleus. The muon experiment (BCDMS) found a much faster falloff  $F_2^C \propto \exp(-16.5x)$ . Of the two high  $Q^2$  experiments the BCDMS data has much lower statistics, while the CCFR experiment has a much poorer resolution in  $x$ , and both experiments have limited  $x$  coverage, making it difficult to directly compare the results. While the measurements were taken on different nuclei, one would expect the carbon and iron structure functions to be very similar, and a *larger* contribution from superfast quarks for iron, due to the small increase in Fermi momentum.

From the E02-019 data, we fit our high  $Q^2$  data for  $1 < \xi < 1.25$  to the form  $F_2^{(0)} \propto \exp -s\xi$  to compare the falloff to the previous measurements. We obtain  $s = 15.0 \pm 0.5$  for carbon, and  $s = 14.1 \pm 0.5$  for copper (our closest nucleus to the CCFR iron target). This shows that the large difference between BCDMS and CCFR is not related to the difference in target nuclei, and that the behavior of the structure function at the present  $Q^2$  values is more consistent with the BCDMS

result. While the E02-019 results support the conclusions of the BCDMS measurement, they are not a high enough  $Q^2$  to allow for a direct extraction of the nuclear pdfs at  $\xi \gtrsim 1$ . Because the BCDMS data are limited to  $\xi < 1.05$ , it is not clear that they have the kinematic reach necessary to test predictions of the high- $\xi$  behavior. In addition, the BCDMS data above  $\xi = 0.65$  appear to have little or no  $Q^2$  dependence, which is not consistent with the expectation that there will be significant impact from QCD evolution at large  $\xi$ .

### B. Sensitivity to Quark Degrees of Freedom in Nuclei

Mapping out the nuclear parton distributions at  $x \gtrsim 1$  is not simply a matter of completing our measurements of pdfs in nucleons and nuclei. They also provide important sensitivity to short range structure in nuclei. The quark distribution at  $x > 1$  is extremely small in a simple convolution model, as the nucleon quark distributions fall rapidly as  $x \rightarrow 1$ , and there are very few fast nucleons available to boost the quarks to  $x > 1$ . The bulk of the strength for  $x \gtrsim 1.1$ – $1.2$  come from the high momentum nucleons generated by short range correlations in nuclei. In addition, this region is extremely sensitive to the behavior of quarks in nucleons at short range; the number of extremely high momentum quarks can be dramatically increased due to the possibility to directly exchange momentum between the quarks in two nucleons (either through q–q scattering in "overlapping" nucleons or the presence of a small 6-quark bag component).

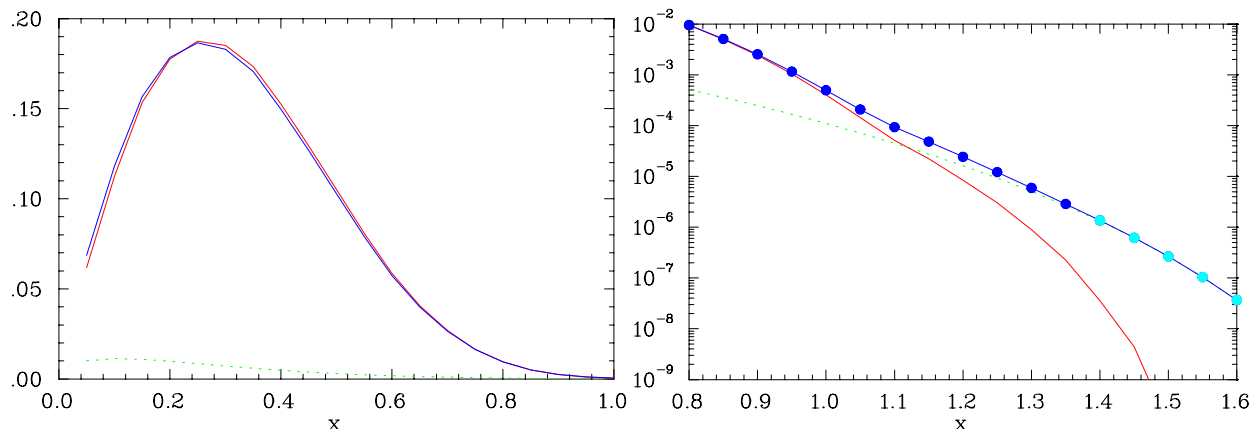


FIG. 4: The deuteron valence quark distributions ( $x < 1$  on the left,  $x > 1$  on the right) from a convolution of proton and neutron quark distributions (red), and with the inclusions of a 5% 6-quark bag component (blue). The dotted green line shows the contribution from the 6-quark bag component. The circles show projected results for the high  $Q^2$  measurements (the uncertainties are smaller than the points). The points at  $x > 1.4$ , shown in dark blue, show the region where the cross section is dominated by DIS, although 6 GeV data suggest that precise scaling extends to larger  $x$  values.

The EMC effect provides clear evidence that the quark distribution in nuclei is not a simple sum of the quark distributions of its constituent protons and neutrons. Many explanations of the EMC effect were proposed which involved non-hadronic degrees of freedom in the nucleus, and measurements of the structure functions at  $x > 1$  provide a unique sensitivity [11, 12, 31] to such models. Figure 4 provides a simple example: It shows the nuclear structure function for deuterium, as calculated from a convolution of neutron and proton structure functions (red), and compares it to the structure function obtained by assuming that 5% of the deuteron wave function is described by a 6-quark bag, using the model of Mulders and Thomas [32] for the quark distribution for the 6-q bag. In the region

of the EMC effect ( $x < 0.8$ ), the difference is at most 2%. However, for  $x > 1$ , the small 6-quark bag component leads to a dramatic increase in the large  $x$  parton distributions, due to the free sharing of momentum between the 6 quarks.

The increase in beam energy to 11 GeV will have the greatest impact on the  $Q^2$  range for kinematic points with  $1.0 \lesssim x \lesssim 1.5$ . This extended  $Q^2$  data is critical to studies of the extremely large  $x$  quark distributions.

#### IV. EXPERIMENTAL DETAILS

While probing different physics than previous measurements, this experiment is, from a technical point of view, a relatively straightforward extension of the lower energy measurements of inclusive scattering from nuclei. The dominant sources of background are the pion contamination of the electron distribution and charge symmetric background. In the previous runs, this contamination was always less than 1% in the HMS when using the calorimeter and Čerenkov information for particle identification. While the pion background will be somewhat worse at these larger energies, the main limitation at lower energies was the pion rejection in the calorimeter when the scattered electron was at low momentum. In this proposal, the minimum scattered electron energy is significantly higher: 1.5 GeV for the HMS, and 4 GeV for the SHMS, and the pion rejection should be sufficient for the proposed kinematics.

The kinematic extent is shown in Fig. 5 where the black (red) crosses indicated the E02-019 (CLAS) kinematics. The blue (solid) symbols and line define the region accessible at 11 GeV. The solid (dashed) blue curve indicates the region where the projected statistical uncertainties are 10% (5%) for an  $x$  bin of 0.05. The labels HMS and SHMS indicate which spectrometers will be used for the different  $Q^2$  and  $x$  ranges. Most of the time, data will be taken simultaneously in both spectrometers.

##### A. Experimental Equipment

The experimental set-up for measurements with a 11 GeV beam would be performed using the existing HMS and the new SHMS which is part of the base equipment package for the 12 GeV upgrade. The HMS would be used for the highest  $Q^2$  measurements at large angles and the SHMS would be used for the intermediate angles,  $\lesssim 30^\circ$  providing the intermediate  $Q^2$  measurements for  $x \lesssim 1.5$ , and the modest  $Q^2$  but very large  $x$  measurements. Data would be taken in the HMS spectrometer using the existing detector package which includes a threshold gas Čerenkov counter and a lead glass shower counter for rejection of pion background. The SHMS will have a similar package of nearly identical performance.

A cryogenic hydrogen target is necessary for calibration and a cryogenic deuterium target for production data. These are currently part of the standard Hall C cryotarget system.  $^3\text{He}$  and  $^4\text{He}$  cells have been used in E02-019, and we found that these cells performed extremely well at currents up to  $80\mu\text{A}$ . Our experience from E02019 with subtraction of the cryogenic cell end caps instructs us to use a longer cell – 8 cm rather than 4 cm. In 2006 we also proposed take data on several solid targets,  $^9\text{Be}$ ,  $^{12}\text{C}$ ,  $^{63}\text{Cu}$ , and  $^{197}\text{Au}$ , which will allow us to measure the  $A$  dependence of the contributions from short range correlations, the  $A$  dependence of the quark distributions at  $x > 1$ ,

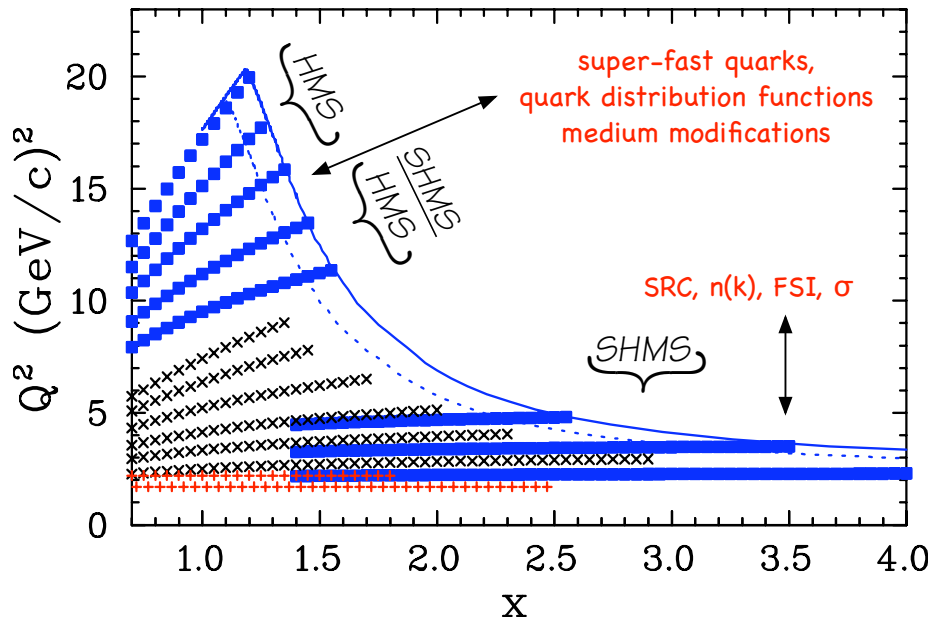


FIG. 5: The kinematic range in  $Q^2$  and the Bjorken  $x$  variable for the already existing data (black), the ratio data from Hall B (red) and the data to be taken in the new experiment (blue). Indicated are the different physics topics that will be emphasized in the different regions along with the spectrometer(s) which will be used in the data taking.

and allow for an extrapolation to nuclear matter. The measurements would be done at several angles to cover the full kinematic range, as shown in Fig. 5.

Motivated in part by the results from E03-103 (EMC in Hall C) that suggests that the size of the EMC effect is generated by the effective density, we will expand the solid target set proposed initially proposed. These would include  ${}^6,7\text{Li}$ ,  ${}^{10,11}\text{B}$  and  ${}^{40,48}\text{Ca}$ . The 11 GeV extension of the EMC experiment (E12-10-008) has also proposed these same targets. Their use in this experiment will be restricted to the large  $x$  and low  $Q^2$  region, as this minimizes the run time required and yields the most relevant physics for these targets. No extra beam time is requested, as the time time saved using the longer cryogenic cells will allow for the inclusion of these targets.

## V. SUMMARY

We propose to measure inclusive scattering at  $x > 1$  on several light and heavy nuclei. The data are broken into two kinematic regions. Data taken at moderate  $Q^2$  values for extremely large  $x$ , where the cross section ratios are sensitive to the presence of two-nucleon and multi-nucleon correlations. The cross section ratios at very large  $x$  will allow us to study in detail the  $A$  dependence of the strength of 2N and 3N SRCs. The coverage should also allow for first studies of the size and importance of  $\alpha$ -clusters in nuclei.

These data will complement the many completed and upcoming coincidence  $A(e, e'p)$  and  $A(e, e'NN)$  measurements attempting to probe the high momentum components of the spectral function and short range correlations [33–35]. The inclusive measurement can reach much larger values of the missing momentum, where the coincidence measurements become cross section (or background) limited. The inclusive measurements are also cleaner, being significantly less sensitive

to final state interactions, meson exchange currents, and other processes which must be modeled in the analysis of the coincidence measurements. In the inclusive measurement, one does not reconstruct the excitation energy of the final system (the missing energy of the struck nucleon), and so is sensitive to the entire missing energy distribution of the spectral function. Both inclusive and coincidence experiments are important in these studies, as inclusive measurements can provide fairly clean information on the very high momentum components of the spectral function, while the coincidence experiments can provide detailed information on the missing energy distribution (and momentum distributions for the individual shells) at lower momentum values.

The second physics goal is the extraction of the structure functions, and thus the unseparated quark distributions, at  $x > 1$ . The existing measurements from neutrino and muon scattering are of limited statistical precision and kinematic coverage, and yield contradictory results. Nuclear dependence of the structure functions at  $x > 1$  can provide new insight into the origin of the EMC effect, and the distribution of these superfast quarks in nuclei is extremely sensitive to non-hadronic components, providing orders of magnitude more sensitivity to configurations such as 6-quark bags.

- 
- [1] J. Arrington, D. Day, et al., <http://www.jlab.org/exp-prog/proposals/06/PR12-06-105.pdf>.
  - [2] D. B. Day et al., Phys. Rev. Lett. **43**, 1143 (1979).
  - [3] D. B. Day et al., Phys. Rev. Lett. **59**, 427 (1987).
  - [4] J. Arrington et al., Phys. Rev. Lett. **82**, 2056 (1999).
  - [5] J. Arrington et al., Phys. Rev. C **64**, 014602 (2001).
  - [6] J. Arrington, D. Day, B. Filippone, A. F. Lung, et al., Jefferson lab experiment E02-019.
  - [7] K. S. Egiyan et al. (CLAS), Phys. Rev. **C68**, 014313 (2003).
  - [8] K. S. Egiyan et al. (CLAS), Phys. Rev. Lett. **96**, 082501 (2006).
  - [9] J. Arrington, R. Ent, C. E. Keppel, J. Mammei, and I. Niculescu, Phys. Rev. **C73**, 035205 (2006).
  - [10] L. L. Frankfurt and M. I. Strikman, Phys. Rept. **160**, 235 (1988).
  - [11] D. F. Geesaman, K. Saito, and A. W. Thomas, Ann. Rev. Nucl. Sci. **45**, 337 (1995).
  - [12] M. M. Sargsian et al., J. Phys. **G29**, R1 (2003).
  - [13] D. B. Day, J. S. McCarthy, T. W. Donnelly, and I. Sick, Ann. Rev. Nucl. Part. Sci. **40**, 357 (1990).
  - [14] L. L. Frankfurt and M. I. Strikman, Nucl. Phys. **B181**, 22 (1981).
  - [15] C. C. degli Atti and S. Simula, Phys. Lett. B **325**, 276 (1994).
  - [16] O. Benhar and S. Liuti, Phys. Lett. B **358**, 173 (1995).
  - [17] O. Benhar, Phys. Rev. Lett. **83**, 3130 (1999).
  - [18] L. L. Frankfurt, M. I. Strikman, D. B. Day, and M. Sargsian, Phys. Rev. **C48**, 2451 (1993).
  - [19] K. Egiyan et al., cLAS-NOTE 2005-004, [www1.jlab.org/ul/Physics/Hall-B/clas](http://www1.jlab.org/ul/Physics/Hall-B/clas).
  - [20] J. Arrington, D. Day, D. Higinbotham, P. Solvignon, et al., Jefferson lab experiment E08-014.
  - [21] D. Day and I. Sick, Phys. Rev. **C69**, 028501 (2004).
  - [22] H. Georgi and H. D. Politzer, Phys. Rev. D **14**, 1829 (1976).
  - [23] O. Nachtmann, Nucl. Phys. **B63**, 237 (1973).
  - [24] N. Fomin et al., in preparation, to be submitted to PRL.
  - [25] I. Schienbein et al., J. Phys. **G35**, 053101 (2008).
  - [26] L. W. Whitlow, E. M. Riordan, S. Dasu, S. Rock, and A. Bodek, Phys. Lett. **B282**, 475 (1992).
  - [27] J. Gomez et al., Phys. Rev. D **49**, 4348 (1994).
  - [28] B. W. Filippone et al., Phys. Rev. C **45**, 1582 (1992).
  - [29] A. C. Benvenuti et al. (BCDMS), Phys. Lett. B **189**, 483 (1987).
  - [30] M. Vakili et al. (CCFR), Phys. Rev. **D61**, 052003 (2000), hep-ex/9905052.
  - [31] M. Arneodo, Phys. Rept. **240**, 301 (1994).
  - [32] P. J. Mulders and A. W. Thomas, Phys. Rev. Lett. **52**, 1199 (1984).
  - [33] D. Rohe et al., Phys. Rev. Lett. **93**, 182501 (2004).
  - [34] M. M. Rvachev et al. (The Jefferson Lab Hall A), Phys. Rev. Lett. **94**, 192302 (2005).
  - [35] W. Bertozzi, E. Piasetzky, J. Watson, S. Wood, et al., Jefferson lab experiment E01-015.